International Journal of Advanced Computer and Mathematical Sciences
ISSN 2230-9624. Vol 3, Issue 4, 2012, pp 471-481
http://bipublication.com

AN ANALYSIS OF NON-UNIFORM HEAT SOURCE FOR THE MAXWELLS FLUID OVER A STRETCHING SHEET WITH VISCOUS DISSIPATION

[1]M. Subhas Abel, [2]Jagadish V. Tawade[*] and [3]Anand H. Agadi

[1]Department of Mathematics, Gulbarga University, Gulbarga- 585 106, Karnataka, INDIA
[2]Department of Mathematics, Walchand Institute of Technology, Solapur-413 006, Maharashtra, INDIA
[3]Department of Mathematics, Basaveshwar Engineering College, Bagalkot-587102, Karnataka, INDIA
* Corresponding author- Email: Jagadishmaths22@gmail.com (Jagadish. V. Tawade).
Tel.: 0217-2653040 (Off), +91-9945118525(Residence), +91-9096544164 (Mobile)

[Received-03/08/2012, Accepted-01/09/2012]

ABSTRACT

In the present work, the effect of non-uniform heat source for the upper convected Maxwells fluid over a stretching sheet with viscous dissipation is examined. The governing boundary layer equations of motion and heat transfer are first non-dimensionalized using suitable similarity variables and the resulting equations are transformed into ordinary differential equations, are then solved numerically by fourth order Runge-Kutta method with efficient shooting technique. For the Maxwells fluid, a thinning of the boundary layer and a drop in wall skin friction coefficient is predicted to occur for higher the elastic number which, agrees with the results of Hayat et.al [24]. Two important heating process are considered namely, i) Prescribed surface temperature (PST-case) and ii) Prescribed heat flux (PHF-case). Several parameter effects have been shown with the aid of graphs. The result obtained for non-uniform heat source with viscous dissipation reveal an interesting behavior in the heat transfer of the fluid.

Keywords Maxwells fluid, Elastic parameter, Prandtl number, Eckert number and non-uniform heat source/sink.

1. INTRODUCTION

Sakiadis [1, 2] has initiated the study of boundary problem assuming velocity of a boundary sheet as constant. Extrusion of molten polymers through a slit die for the production of plastic sheets is an important process in polymer industry. The operation normally involves significant heat transfer between the sheet and the surrounding fluid thus making it a difficult thermo-fluid problem to address [3]. In a typical sheet production process the extrudate starts to solidify as soon as it exits from the die. The sheet is then collected by a wind-up roll upon solidification (see fig. 1). An important aspect of the flow is the extensibility of the sheet which can be employed effectively to improve its mechanical properties

along the sheet. To further improve sheet mechanical properties, it is necessary to control its cooling rate. Physical properties of the cooling medium e.g., its thermal conductivity, can play a decisive role in this regard [3]. The success of the whole operation can be argued to depend also on the rheological properties of the fluid above the sheet as it is the fluid viscosity which determines the (drag) force required to pull the sheet.

In reality most liquids are non-Newtonian in nature, which are abundantly used in many industrial applications, such as in the manufacture of plastic films and artificial fibers, aerodynamic extrusion of plastic sheets, cooling of metallic sheets in a cooling path, crystal growing, liquid film condensation process, continuous polymer sheet extrusion, heat treated materials travelling between a feed roll, wind up roll or on a conveyer belt, geothermal reservoirs and petroleum industries.

Water is amongst the most widely used fluids to be used as the cooling medium. However, the rate of cooling achievable with water is often realized to be too excessive for certain sheet materials. To have a better control on the rate of cooling , in recent years it has been proposed that it might be advantageous for water to be made more or less viscoelastic, say, through the use of polymeric additives[7, 8]. The idea is to alter flow kinematics in such a way that it leads to a slower rate of solidification with the price being paid that fluid's viscosity is normally increased by such additives. A better and less intrusive idea is to rely on a transverse magnetic field for affecting flow kinematics provided the fluid is electrically conducting [4].

The radioactive heat transfer properties of the cooling medium may also be manipulated to judiciously influence the rate of cooling [5, 6]. Obviously, one can also envisage cases in which a combination of different methods can be used in order to obtain the best results. To better understand the effects of such parameters on different aspects of the flow much study has been carried out in the past on stretching sheets.

The study of visco-elastic boundary layer flow problem has been further channelized to non-Newtonian fluid flow. Review of literature reveals that Rajgopal et.al [8] have considered the study of visco-elastic second order fluid flow over a stretching sheet by solving boundary layer equations numerically, this work does not take in to account of the heat transfer phenomenon. Siddappa and Abel [21] have considered similar flow analysis without heat transfer in the flow of non-Newtonian fluid of Walters liquid. Bujurke et. al [9] have presented work to analyze momentum and heat transfer phenomena in visco-elastic second order fluid over a stretching sheet with internal heat generation and viscous dissipation.

Crane [10] was the first among the others to consider the steady two-dimensional flow of a Newtonian fluid driven by a stretching elastic flat sheet which moves in its own plane with a velocity varying linearly with the distance from a fixed point. Subsequently, various aspects of the flow and/or heat transfer problems for stretching surfaces moving in the finite fluid medium have been explored in many investigations e.g. Ref [11-15]

Hayat et.al [22] studied the MHD stagnation-point flow of UCM fluid over stretching sheet. The researchers [23,24,26] have worked on the Maxwells fluid by using homotopy analysis method and the researcher [25] have discussed the effect of stagnation-point flow of upper convected Maxwell fluid analytically by using Chebyshev pseudo-spectral collocation-point method with no heat transfer. Motivating by all the above work, it is recognized that there are many other methods that could be considered in order to describe some reasonable solutions for this particular type of problems but to the best of our knowledge, no numerical solution has previously been investigated for the combined effect of non-uniform heat source/sink and

viscous dissipation for the Maxwells fluid over a stretching sheet.

2. Mathematical formulation of the problem

The equations governing the transfer of heat and momentum between a stretching sheet and the surrounding fluid (see fig.1) can be significantly simplified if it can be assumed that boundary layer approximations are applicable to both momentum and energy equations. Although this theory is incomplete for viscoelastic fluids, but has been discussed by Renardy [29], it is more plausible for Maxwell fluids as compared to other viscoelastic fluid models for MHD flow of an incompressible Maxwell fluid resting above a stretching sheet. The steady two-dimensional boundary layer equations for the fluid can be written as [30, 31]

$$\frac{\partial u}{\partial x}+\frac{\partial v}{\partial y}=0, \tag{1}$$

$$u\frac{\partial u}{\partial x}+v\frac{\partial u}{\partial y}+\lambda\left[u^2\left(\frac{\partial^2 u}{\partial x^2}\right)+v^2\left(\frac{\partial^2 u}{\partial y^2}\right)+2uv\left(\frac{\partial^2 u}{\partial x\partial y}\right)\right]=\upsilon\left(\frac{\partial^2 u}{\partial y^2}\right), \tag{2}$$

Where υ is the kinematic viscosity of the fluid and λ is the relaxation time Parameter of the fluid. As to the boundary conditions, we are going to assume that the sheet is being stretched linearly. Therefore the appropriate boundary conditions on the flow are

$$u=Bx, \quad v=0 \ \text{ at } \ y=0, \qquad u\to 0 \ \text{ as } \ y\to\infty \tag{3}$$

Where B>0, is the stretching rate. Here x and y are, respectively, the directions along and perpendicular to the sheet, u and v are the velocity components along x and y directions. The flow is caused solely by the stretching of the sheet, the free stream velocity being zero. Equations (1) and (2) admit a self-similar solution of the form

$$u=Bxf'(\eta), \quad v=\sqrt{\nu B}\,f(\eta), \quad \eta=\left(\frac{B}{\nu}\right)^{\frac{1}{2}}y, \tag{4}$$

Where superscript ' denotes the differentiation with respect to η. Clearly u and v satisfy equation (1) identically. Substituting these new variables in Eq. (2), we have

$$f'''-(f')^2+ff''+\beta\left(2ff'f''-f^2f'''\right)=0, \tag{5}$$

Here $\beta=\lambda B$ is the elastic parameter.

The boundary conditions (3) become

$$f'(\eta)=1, \quad f(\eta)=0 \quad \text{at} \quad \eta=0$$
$$f'(\eta)\to 0, \quad f''(\eta)\to 0 \quad \text{as} \quad \eta\to\infty \tag{6}$$

3. Heat transfer analysis

By using usual boundary layer approximations, the equation of the energy for two-dimensional flow is given by

$$\rho C_p\left(u\frac{\partial T}{\partial x}+v\frac{\partial T}{\partial y}\right)=k\frac{\partial^2 T}{\partial y^2}+\mu\left(\frac{\partial u}{\partial y}\right)^2+q''' \tag{7}$$

where T, ρ, C_p, q''' and k are, respectively, the temperature, the density, specific heat at constant pressure, space and temperature dependent internal heat generation/absorption (non-uniform heat source/sink) and the thermal conductivity is assumed to vary linearly with temperature. q''' can be expressed in simplest form as (as referred in [16-20, 28])

$$q'''=\frac{ku_w(x)}{x\upsilon}[A^*(T_w-T_\infty)f_\eta'+B^*(T-T_\infty)]$$

Where A* and B* are coefficient of the space and temperature dependent internal heat generation / absorption. The case A* >0 and B*>0 corresponds to internal heat generation while A* < 0 and B* < 0 correspond to internal absorption. The solution of Eq. (7) depends on the nature of the prescribed boundary conditions.

We define the dimensionless temperature as

$$\theta(\eta)=\frac{T-T_\infty}{T_w-T_\infty},\ \text{where}\ T_w-T_\infty=b\left(\frac{x}{l}\right)^2\ \theta(\eta) \qquad (PST\ Case) \tag{8}$$

$$g(\eta)=\frac{T-T_\infty}{b\left(\frac{x}{l}\right)^2\frac{1}{k}\sqrt{\frac{\nu}{b}}},\ \text{where}\ T_w-T_\infty=\frac{D}{k}\left(\frac{x}{l}\right)^2\sqrt{\frac{\upsilon}{b}} \qquad (PHFC\ case) \tag{9}$$

The thermal boundary conditions depend upon the type of the heating process being considered. Here, we are considering two general cases of heating namely, (1) Prescribed surface temperature and (2) prescribed wall heat flux, varying with the distance.

3.1. *Governing equation for the prescribed surface temperature case*

For this heating process, the prescribed temperature is assumed to be a quadratic function of x and is given by

$$u=Bx,\ v=0,\quad T=T_w(x)=T_0-T_s\left(\frac{x}{l}\right)^2 \quad at\ y=0.$$
$$u=0,\qquad T\to T_\infty \qquad as \quad y\to\infty \tag{10}$$

where l is the characteristic length. Using (4), (7) and (10), the dimensionless temperature variable θ given by (8), satisfies

$$\Pr\left[2f'\theta-\theta'f-Ecf''^2\right]=\theta''-(A^*f'+B^*\theta), \tag{11}$$

Where $\Pr=\dfrac{\mu c_p}{k}$ is the Prandtl number, $Ec=\dfrac{a^2l^2}{C_pT_s}$ is the Eckert number, A^* and B^* are space and temperature dependent internal heat generation / absorption.

The corresponding boundary conditions are

$$\theta(\eta)=1 \quad \text{at} \quad \eta=0$$
$$\theta(\eta)\to 0 \quad as \quad \eta\to\infty \tag{12}$$

3.2. *Governing equation for the prescribed heat flux case*

The power law heat flux on the wall surface is considered to be a quadratic power of x in the form

$$u=Bx,\quad -k\left(\frac{\partial T}{\partial y}\right)_w=q_w=b\left(\frac{x}{l}\right)^2 \quad at \quad y=0$$
$$u\to 0,\quad T\to T_\infty \quad as \quad y\to\infty. \tag{13}$$

Here D is constant. Using (4), (7) and (13), the dimensionless temperature variable g(η) given by (9), satisfies

$$\Pr\left[2f'g-g'f-Ecf''^2\right]=g''-(A^*f'+B^*g) \tag{14}$$

The corresponding boundary conditions are

$$g'(\eta)=-1\ at\ \eta=0.\quad g(\eta)\to 0\ as\ \eta\to\infty. \tag{15}$$

The rate of heat transfer between the surface and the fluid conventionally expressed in dimensionless form as a local Nusselt number and is given by

$$Nu_x\equiv-\frac{x}{T_w-T_\infty}\left(\frac{\partial T}{\partial y}\right)_{y=0}=-x\sqrt{\mathrm{Re}}\ \theta'(0) \tag{16}$$

Similarly, momentum equation is simplified and exact analytic solutions can be derived for the skin-friction coefficient or frictional drag coefficient as

$$C_f\equiv\frac{\left(\mu\dfrac{\partial u}{dy}\right)_{y=0}}{\rho(Bx)^2}=-f''(0)\frac{1}{\sqrt{\mathrm{Re}_x}} \tag{17}$$

where $\mathrm{Re}_x=\dfrac{\rho Bx^2}{\mu}$ is known as local Reynolds number.

4. Numerical solution

We adopt the most effective shooting method (see Refs. [32, 33]) with fourth order Runge-Kutta integration scheme to solve boundary value problems in PST and PHF cases mentioned in the previous section. The non-linear equations (5) and (11) in the PST case are transformed into a system of five first order differential equations as follows:

$$\frac{df_0}{d\eta} = f_1,$$

$$\frac{df_1}{d\eta} = f_2,$$

$$\frac{df_2}{d\eta} = \frac{(f_1)^2 - f_0 f_2 - 2\beta f_0 f_1 f_2}{1-\beta f_0^{\,2}},$$

$$\frac{d\theta_0}{d\eta} = \theta_1,$$

$$\frac{d\theta_1}{d\eta} = \Pr\left[2 f_1\theta_0 - \theta_1 f_0 - Ecf''^{2}\right] + (A^* f' + B^*\theta). \tag{18}$$

Subsequently the boundary conditions in (6) and (16) take the form,

$$f_0(0) = 0, \quad f_1(0) = 1, \quad f_1(\infty) = 0,$$
$$f_2(0) = 0, \quad \theta_0(0) = 0, \quad \theta_0(\infty) = 0. \tag{19}$$

Here $f_0 = f(\eta)$ and $\theta_0 = \theta(\eta)$, aforementioned boundary value problem is first converted into an initial value problem by appropriately guessing the missing slopes $f_2(0)$ and $\theta_1(0)$. The resulting IVP is solved by shooting method for a set of parameters appearing in the governing equations with a known value of $f_2(0)$ and $\theta_1(0)$. The convergence criterion largely depends on fairly good guesses of the initial conditions in the shooting technique. The iterative process is terminated until the relative difference between the current iterative values of $f_2(0)$ matches with the previous iterative value of $f_2(0)$ up to a tolerance of 10^{-6}. Once the convergence is achieved we integrate the resultant ordinary differential equations using standard fourth order Runge–Kutta method with the given set of parameters to obtain the required solution.

5. Results and Discussion

The non-linear coupled ordinary differential equations (5), (11) and (14) subject to the boundary conditions (6), (12) and (15) were solved numerically using the most effective numerical fourth-order Runge-Kutta method with efficient shooting technique. Appropriate similarity transformation is adopted to transform the governing partial differential equations of flow and heat transfer into a system of non-linear ordinary differential equations. In order to validate the numerical method, comparison with the exact analytical solutions for the local skin-friction and the local Nusselt number are shown in Table 1 and 2. Without any doubt, from these tables we can claim that our results are in excellent agreement with that of references Hayat et.al [25], Sadeghy et.al [26] and Aliakbar et.al [27] under some limiting cases. The effects of surface temperature $\theta(1)$ and heat transfer rate $-\theta'(0)$ for various values of *Pr*, *Ec*, A^*, B^* and β are tabulated in Table 3. The effect of several parameters controlling the velocity and temperature profiles are shown graphically and discussed briefly.

Figs. 2 and 3 show the effects of Elastic parameter β on the velocity profiles above the sheet. An increase in the elastic number β is seen to decrease both u- and v-velocity components at any given point above sheet. A decrease in a stream-wise velocity component, u, can result in a decrease in the amount of heat transferred from the sheet to the fluid. Similarly, a decrease in the transverse velocity component, v, means that the amount of fresh fluid which is extended from the low-temperature region outside the boundary layer and directed towards the sheet is reduced thus decreasing the amount of heat transfer. The

two effects are in the same direction reinforcing each other. Thus, an increase in the elastic number is expected to decrease the total amount of heat transfer from the sheet to the fluid, as suggested by Figs. 4 &5. That is, an increase in the elastic number decreases fluid temperature at any given point above the sheet.

Figs.6 and 7 show the effect of Prandtl number on the temperature profiles above the sheet for both PST and PHF cases. An increase in the Prandtl number is seen to decrease the fluid temperature $\theta(\eta)$ above the sheet. That is not surprising realizing the fact that the thermal boundary becomes thinner for, larger the Prandtl number. Therefore, with an increase in the Prandtl number the rate of thermal diffusion drops. This scenario is valid for both PST and PHF cases. For the PST case the dimensionless wall temperature is unity for all parameter values. However, it may be other than unity for the PHF case because of its differing thermal boundary conditions.

Figs. 8and 9 show the effect of Eckert number on the temperature profiles above the sheet for both PST and PHF cases. An increase in the value of Eckert number is seen to increase the temperature of the fluid at any point above the sheet.

Figs. 10 and 11 are the graphs of temperature profiles $\theta(\eta)$ and $g(\eta)$ verses distance η, for different values of A^*. For $A^*>0$, it can be seen that the thermal boundary layer generates the energy, and this causes the temperature $\theta(\eta)$ and $g(\eta)$ of the fluid to increase with increase in the value of $A^*>0$ (heat source), where as for $A^*<0$ (absorption) the temperature $\theta(\eta)$ decreases with the increase in the value of A^*.

Figs. 12 and 13 depict the temperature profiles $\theta(\eta)$ and $g(\eta)$ verses distance η, for different values of B^*. The explanation on the effect of B^* is similar to that given for A^*.

6. CONCLUSIONS

The present work analyses, the effect of non-uniform heat source for the Maxwells fluid over a stretching sheet. Numerical results are presented to illustrate the details of the flow and heat transfer characteristics and their dependence on the various parameters.

1. We observe that, when the elastic parameter increases, there is a decrease in velocity. The effect of Elastic parameter on the Maxwells fluid over the stretching sheet is to suppress the velocity field, which in turn causes the enhancement of the temperature field.
2. Also it is observed that, an increase of Prandtl number results in decreasing thermal boundary layer thickness and more uniform temperature distribution across the boundary layer in both the PST and PHF cases. The reason is that smaller values of *Pr* are equivalent to increasing the thermal conductivities, and therefore heat is able to diffuse away from the heated surface more rapidly than for higher values of *Pr*.
3. An increase in the Eckert number causes an increase in the temperature of the fluid above the sheet. Thus, it may be used to reduce the rate of cooling. For the PST case, fluid temperature near the wall is predicted to exceed wall temperature inferring that the direction of heat transfer is reversed from the fluid to the sheet.
4. The effect of non-uniform heat source/sink parameter is to generate temperature for increasing positive values and absorb temperature for decreasing negative values. Hence non-uniform heat sinks are better suited for cooling purpose.

REFERENCES:

1. B C Sakiadis, Boundary layer behavior on continuous solid surfaces: I Boundary layer equations for two dimensional and axisymmetric flow, AIChE J. 7(1961)26-28.
2. B C Sakiadis, Boundary layer behavior on continuous solid surfaces: II Boundary layer on a

continuous flat surface, AIChE. J. 7(1961)221-225.
3. A. Raptis, Radiation and viscoelastic flow. Int Commun Heat Mass Transfer. 26(6)(1999) 889-895
4. D. N. Schulz, J. E. Glass, editors. Polymers as rheology modifiers. ACS symposium series, 462. Washington (DC): American Chemical Society; 1991
5. A. Raptis, C. Perdikis, Viscoelastic flow by the presence of radiation. ZAMM. 78(4)(1998), 277-279
6. JF Agassant, P. Avens, J. Sergent, PJ Carreau, Polymer processing: principles and modelling. Munich: Hanser Publishers; 1991
7. H. I. Andersson, Note: MHD flow of a viscoelastic fluid past a stretching surface. Acta Mech. 95 (1992) 227-230
8. K R. Rajgopal, T Y Na, A S Gupta, Flow of a viscoelastic fluid over a sretching sheet. Rheol Acta 23(1984) 213-215.
9. N M Bujurke, S N Biradar, P S Hiremath, Second order fluid flow past a stretching sheet with heat transfer, Z Amp 38(1987) 890-892.
10. L.J. Crane, flow past a stretching plate, Z. Angrew. Math. Phys. 21 (1970) 645-647.
11. L.G. Grubka, K.M, Bobba, Heat Transfer characteristics of a continuous stretching surface with variable temperature, J. Heat Transfer 107 (1985) 248-250.
12. B.K. Dutta, A.S. Gupta, cooling of a stretching sheet in a various flow, Ind. Eng. Chem. Res. 26 (1987) 333-336.
13. D.R. Jeng, T.C.A. Chang, K.J. Dewitt, Momentum and heat transfer on a continuous surface, ASME J. Heat Transfer 108 (1986) 532-539.
14. N. Afzal, Heat transfer from a stretching surface, Int. J. Heat and Mass Transfer 36 (1993) 1128-1131.
15. K.V. Prasad, S. Abel, P.S. Datti, Diffusion of chemically reactive species of a non-Newtonian fluid immersed in a porous medium over a stretching sheet, Int. J. Non-linear Mech. 38 (2003) 651-657.
16. M.S. Abel, P.G. Siddheshwar, Mahantesh M. Nandeppanavar, Heat transfer in a viscoelastic boundary layer flow over a stretching sheet with viscous dissipation and non-uniform heat source. Int. J. Heat Mass Transfer, 50(2007), 960-966.
17. M.S. Abel, Mahantesh M. Nandeppanavar . Effects of radiation & non uniform heat source on MHD flow of Visco-elastic fluid and heat transfer over a stretching sheet. Int J Applied Mech. Eng 2008: 13(2):293-309.
18. M.S. Abel and Mahantesh M. Nandeppanavar, Heat transfer in MHD viscoelastic boundary layer flow over a stretching sheet with space and temperature dependent heat source. Int J Applied Mech. Eng 2008: 13(2):293-309.
19. M.S. Abel and Mahantesh M. Nandeppanavar, Heat transfer in MHD viscoelastic boundary layer flow over a stretching sheet with non uniform heat source/sink. Commun Non-linear Sci Numer Simulat 2009:14:2120-31.
20. M.S. Abel and N.Mahesha, Heat transfer in MHD viscoelastic fluid over a stretching sheet with variable thermal conductivity, non-uniform heat source and radiation, Applied Mathematical Modeling. 32 (10) (2008) 1965-1983.
21. B Siddappa, S Abel, Non-Newtonian flow past a stretching plate, ZAMP 36(1985) 890-892.
22. T. Hayat, Z. Abbas, M. Sajid (2009) MHD Stagnation point flow of an UCM fluid over a stretching sheet. Chaos solutions Fractals 39:840-848.
23. Alizadeh-Pahlavan A, Sadeghy K (2009) on the use of homotopy analysis method for solving unsteady MHD flow of Maxwellian fluids above impulsively stretching sheet. Commun Nonlinear Sci Numer Simul 14(4): 1355-1365.
24. T. Hayat, Z. Abbas, M. Sajid. Series solution for the upper-convected Maxwell fluid over a porous stretching plate. Phys Lett A 358 (2006) 396-403
25. Sadeghy K Hajibaygi H Taghavi S-M(2006) stagnation point flow of UCM fluids. Int J Non-linear Mech. 41: 1242-1247.
26. Aliakbar V, Alizadeh-Pahlavan A, Sadeghy K (2009) The influence of thermal radian on MHD flow of Maxwellian fluids above stretching sheets. Commun Nonlinear Sci Numer Simul 14(3):779-794.
27. M. Renardy. High Weissenberg number boundary layers for the Upper Convected Maxwell fluid. J. Non-Newtonian Fluid Mech. 68 (1997) 125.
28. Emad m. Abo-Eladahab, Mohamed A, El Aziz, Blowing/suction effect on hydromagnetic heat

transfer by mixed convection from an inclined continuously stretching surface with internal heat generation /absorption, Int. J. Therm. Sci. 43 (2004) 709-719

29. M. Renardy. High Weissenberg number boundary layers for the Upper Convected Maxwell fluid. J. Non-Newtonian Fluid Mech. 68 (1997) 125.
30. K. Sadeghy, A.H.Najafi, M.Saffaripour. Sakiadis flow of an upper convected Maxwell fluid Int J Non-Linear Mech 40 (2005) 1220.
31. A. Alizadeh-Pahlavan, V. Aliakbar, F. Vakili-Farahani, K. Sadeghy. MHD flows of UCM fluids above porous stretching sheets using two-axillary-parameter homotopy analysis method. Commun. Ninlinear Sci Numer Simulat, doi:10. 1016/ j.cnsns. 2007. 09.011
32. S.D. Conte, C. de Boor, Elementary Numerical analysis, McGraw-Hill, New York, 1972.
33. T. Cebeci, P. Bradshaw, Physical and computational aspects of convective heat transfer, Springer-Verlag, New York, 1984.

Nomenclature:

b	stretching rate $[s^{-1}]$
x	horizontal coordinate [m]
y	vertical coordinate [m]
u	horizontal velocity component $[m\ s^{-1}]$
v	vertical velocity component $[m\ s^{-1}]$
T	temperature [K]
t	time [s]
C_p	specific heat $[J\ kg^{-1}\ K^{-1}]$
f	dimensionless stream function,
Pr	Prandtl number, $\frac{\upsilon}{k}$
Ec	Eckert number, $\frac{a^2 l^2}{C_p T_s}$
q	heat flux, $-k\frac{\partial T}{\partial y}$ $[J\ s^{-1} m^{-2}]$
Nu_x	local Nusselt number, Eq. (16)
C_f	skin friction coefficient, Eq. (17)
A*	space dependent
B*	temperature dependent

Greek symbols

β	Elastic parameter
η	similarity variable, Eq. (4)
θ	dimensionless temperature,
k	thermal diffusivity $[m^2\ s^{-1}]$
μ	dynamic viscosity $[kg\ m^{-1}\ s^{-1}]$
υ	kinematic viscosity $[m^2\ s^{-1}]$
ρ	density $[kg\ m^{-3}]$
τ	shear stress, $\mu\ \partial u/\partial y$ $[kg\ m^{-1}s^{-2}]$
ψ	stream function $[m^2\ s^{-1}]$

Subscripts

x	local value

Superscripts

'	first derivative
"	second derivative
'''	third derivative

Tables and graphs:

Table 1:
Comparison of values of skin friction coefficient $-f''(0)$ with *M*= 0.0

β	**Sadeghy et.al [25]**	**Hayat et. al [24]**	**Present Results**
	M=0.0	*M=0.0*	*M=0.0*
0.0	1.00000	1.90250	0.999962
0.4	1.10084	2.19206	1.101850
0.8	1.19872	2.50598	1.196692
1.2	-	2.89841	1.285257
1.6	-	3.42262	1.368641
2.0	-	4.13099	1.447617

Table 2:
Comparison of values of of Eckert number *Ec* and Magnetic parameter *Mn* in PST case
$(\lambda = 0.1,\ Pr = 3, A^* = B^* = 0.1)$

Ec	*Mn*	**Aliakbar et. al [26]**	**Present Results**
		$-\theta'(0)$	$-\theta'(0)$
0.0	*0.0*	2.4711€	1.227050
5.0	*0.0*	−1.3880€	−0.718811
10.0	*0.0*	−5.24982	−2.665283

Table 3: Values of surface temperature $\theta(1)$ and heat transfer rate $-\theta'(0)$ for various values of *Pr*, *Ec*, *A**, *B** and β .

Pr	*Ec*	*A**	*B**	β	$\theta(1)$	$\theta'(0)$
1.0	0.2	0.1	0.1	0.1	0.000000	-1.149181
5.0	0.2	0.1	0.1	0.1	-0.000001	-2.972452
10.0	0.2	0.1	0.1	0.1	-0.000001	-4.244381
1.0	1.0	0.1	0.1	0.1	0.000000	-0.837849
1.0	2.0	0.1	0.1	0.1	-0.000001	-0.448684
1.0	5.0	0.1	0.1	0.1	-0.000001	0.718811
1.0	0.2	-0.1	0.1	0.1	0.000000	-1.265852
1.0	0.2	0.0	0.1	0.1	0.000000	-1.207517
1.0	0.2	0.1	0.1	0.1	0.000000	-1.149181
1.0	0.2	0.1	-0.1	0.1	0.000000	-1.252833
1.0	0.2	0.1	0.0	0.1	0.000000	-1.203614
1.0	0.2	0.1	0.1	0.1	0.000000	-1.149181
1.0	0.2	0.1	0.1	0.0	-0.000000	-1.163281
1.0	0.2	0.1	0.1	0.1	-0.000000	-1.149184
1.0	0.2	0.1	0.1	0.3	-0.000000	-1.121014

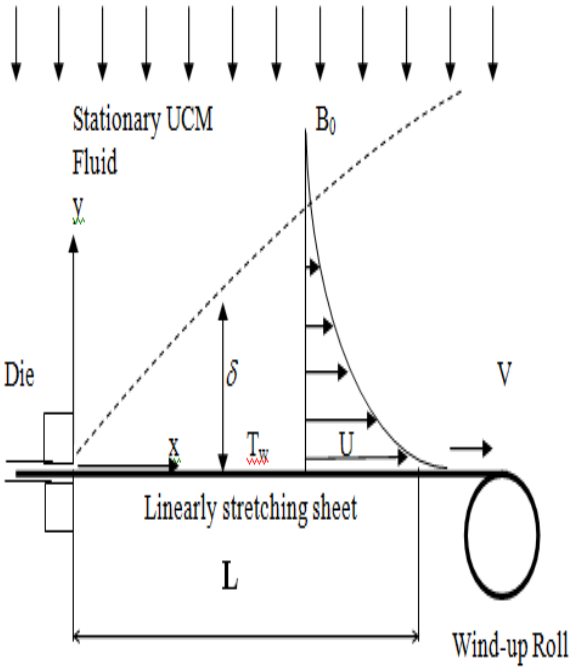

Fig.1. Schematic showing flow above a stretching sheet

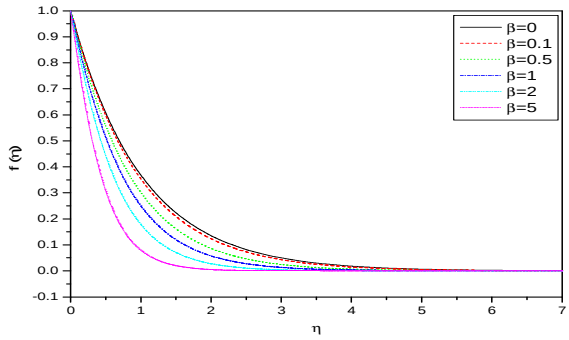

Fig 2 The effect of elastic parameter β on u-velocity component f

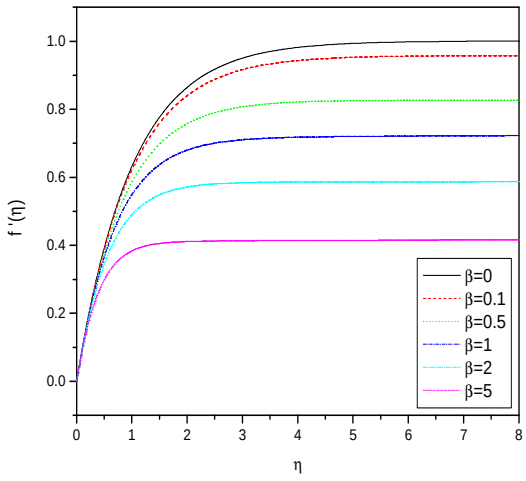

Fig 3 The effect of elastic parameter β on v-velocity component f'

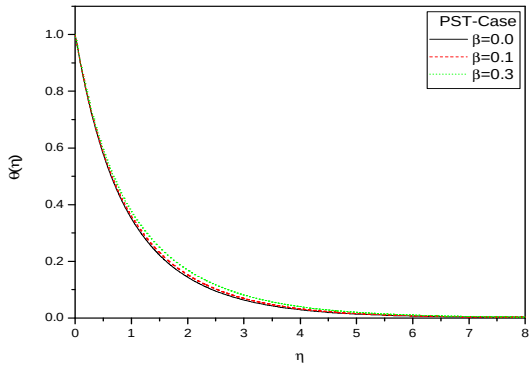

Fig 4 The effect of elastic parameter β on temperature profile for the PST case at

$\Pr = 1.0,\ Ec = 0.2, A^* = B^* = 0.1$

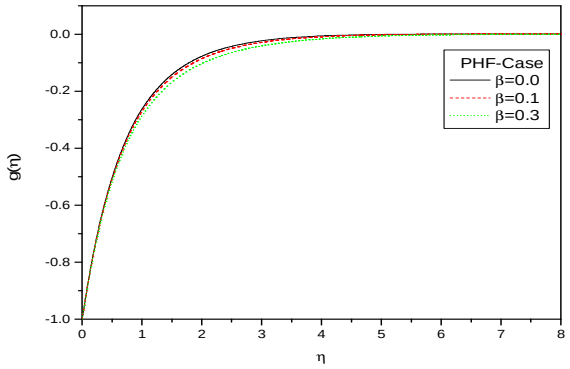

Fig 5 The effect of elastic parameter β on temperature profile for the PHF case at

$$\Pr = 1.0,\ Ec = 0.2, A^* = B^* = 0.1$$

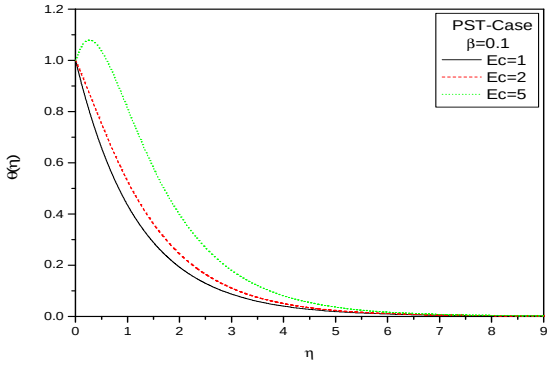

Fig 8 The effect of Eckert number Ec on the temperature profile for the PST case at

$$\beta = 0.1,\ \Pr = 1, A^* = B^* = 0.1$$

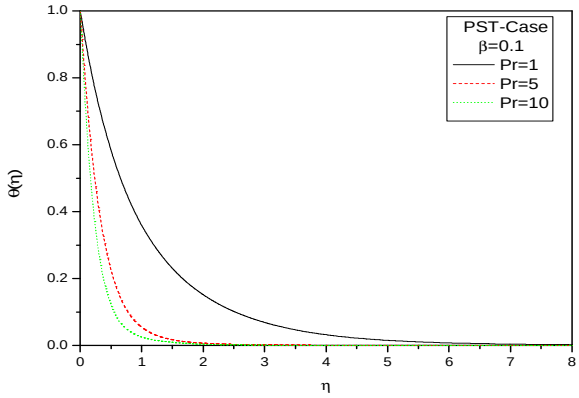

Fig 6 The effect of Prandtl number $\Pr$ on the temperature profile for the PST case at

$$\beta = 0.1,\ Ec = 0.2, A^* = B^* = 0.1$$

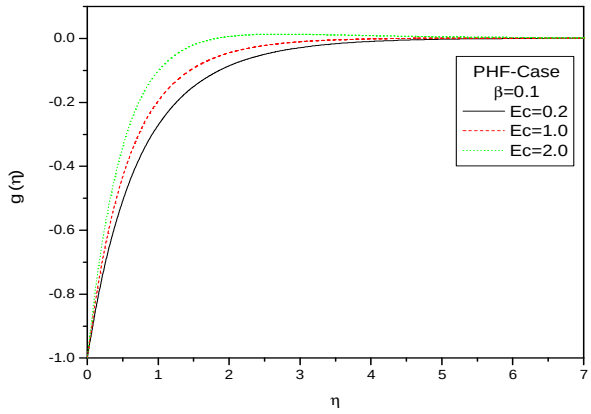

Fig 9. The effect of Eckert number Ec on the temperature profile for the PHF case at

$$\beta = 0.1,\ \Pr = 1, A^* = B^* = 0.1$$

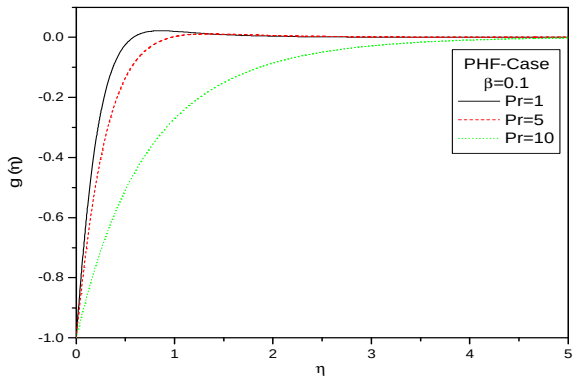

Fig 7 The effect of Prandtl number $\Pr$ on the temperature profile for the PHF case at

$$\beta = 0.1, Ec = 0.2, A^* = B^* = 0.1$$

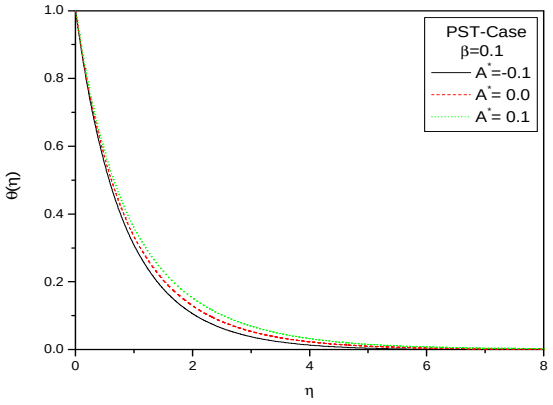

Fig.10 The effect of heat generation A* on the temperature profile for the PST case at

$$\beta = 0.1, \Pr = 1, Ec = 0.2, B^* = 0.1$$

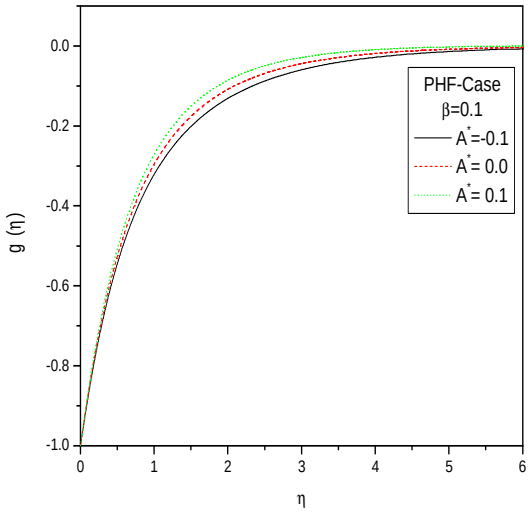

Fig 11. The effect of heat generation A* on the temperature profile for the PHF case at

$$\beta = 0.1, \Pr = 1, Ec = 0.2, B^* = 0.1$$

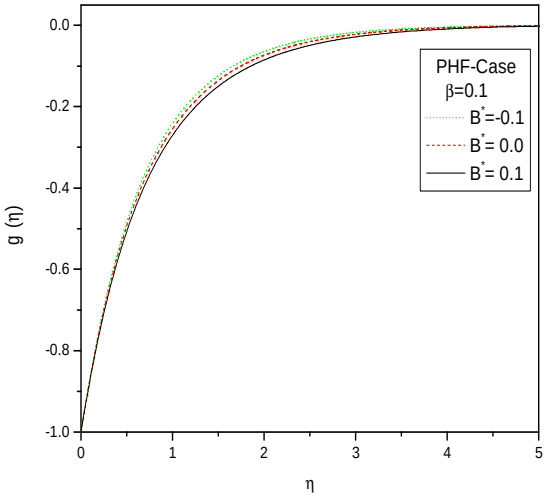

Fig 13. The effect of heat absorption B* on the temperature profile for the PHF case at

$$\beta = 0.1, \Pr = 1, Ec = 0.2, A^* = 0.1$$

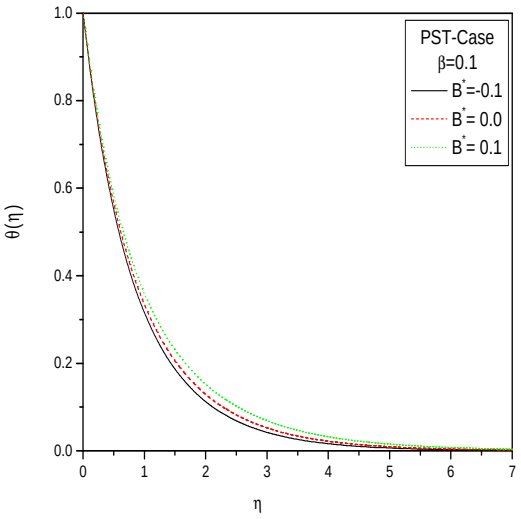

Fig.12 The effect of heat absorption B* on the temperature profile for the PST case at

$$\beta = 0.1, \Pr = 1, Ec = 0.2, A^* = 0.1$$